The Rotational Spectra, Structure, Internal Dynamics, and Electric Dipole Moment of the Argon–Ketene van der Waals Complex

ARTICLE *in* JOURNAL OF MOLECULAR SPECTROSCOPY · JUNE 2001

Impact Factor: 1.48 · DOI: 10.1006/jmsp.2001.8351 · Source: PubMed

7 AUTHORS, INCLUDING:

R.D. Suenram
University of Virginia
247 PUBLICATIONS **6,712** CITATIONS
SEE PROFILE

Francis J. Lovas
National Institute of Standards and Te…
287 PUBLICATIONS **9,068** CITATIONS
SEE PROFILE

Heaven Warner
Northeastern University
35 PUBLICATIONS **269** CITATIONS
SEE PROFILE

Journal of Molecular Spectroscopy **207,** 201–210 (2001)
doi:10.1006/jmsp.2001.8351, available online at http://www.idealibrary.com on IDEAL®

The Rotational Spectra, Structure, Internal Dynamics, and Electric Dipole Moment of the Argon–Ketene van der Waals Complex

C. W. Gillies,* J. Z. Gillies,† S. J. Amadon,† R. D. Suenram,‡ F. J. Lovas,‡ H. Warner,* and R. Malloy*

*Department of Chemistry, Rensselaer Polytechnic Institute, Troy, New York 12180; †Department of Chemistry, Siena College, Loudonville, New York 12111; and ‡Optical Technology Division, National Institute of Standards, Gaithersburg, Maryland 20899

Received December 19, 2000; in revised form March 8, 2001

Pulsed-beam Fourier transform microwave spectroscopy was used to observe and assign the rotational spectra of the argon–ketene van der Waals complex. Tunneling of the hydrogen or deuterium atoms splits the *a*- and *b*-type rotational transitions of H_2CCO–Ar, $H_2{}^{13}CCO$–Ar, $H_2C^{13}CO$–Ar, and D_2CCO–Ar into two states. This internal motion appears to be quenched for HDCCO–Ar where only one state is observed. The spectra of all isotopomers were satisfactorily fit to a Watson asymmetric top Hamiltonian which gave $A = 10\,447.9248(10)$ MHz, $B = 1918.0138(16)$ MHz, $C = 1606.7642(15)$ MHz, $\Delta_J = 16.0856(70)$ kHz, $\Delta_{JK} = 274.779(64)$ kHz, $\Delta_K = -152.24(23)$ kHz, $\delta_J = 2.5313(18)$ kHz, $\delta_K = 209.85(82)$ kHz, and $h_K = 1.562(64)$ kHz for the A_1 state of H_2CCO–Ar. Electric dipole moment measurements determined $\mu_a = 0.417(10)\times10^{-30}$ C m [0.125(3) D] and $\mu_b = 4.566(7)\times10^{-30}$ C m [1.369(2) D] along the *a* and *b* principal axes of the A_1 state of the normal isotopomer. A least squares fit of principal moments of inertia, I_a and I_c, of H_2CCO–Ar, $H_2{}^{13}CCO$–Ar, and $H_2C^{13}CO$–Ar for the A_1 states give the argon–ketene center of mass separation, $R_{cm} = 3.5868(3)$ Å, and the angle between the line connecting argon with the center of mass of ketene and the C=C=O axis, $\theta_{cm} = 96.4^\circ(2)$. The spectral data are consistent with a planar geometry with the argon atom tilted toward the carbonyl carbon of ketene by 6.4° from a T-shaped configuration.

Key Words: Argon–ketene; microwave; spectra.

I. INTRODUCTION

The rotational spectrum of the H_2CCO–Ar complex was first observed in studies of molecular complexes of ketene bound to acetylene and ethylene, H_2CCO–C_2H_2 and H_2CCO–C_2H_4 (*1, 2*). Interest in the structure and internal motions of H_2CCO–Ar stems from recent microwave (*3*) and *ab initio* (*4*) investigations of the related H_2CO–Ar complex. The potential energy surface of H_2CO–Ar calculated by MP2 perturbation theory has a global minimum with the argon atom located in the molecular plane of formaldehyde and tilted toward the oxygen (*4*). The C–O bond is found to be electron-deficient with the electron density being lower in the molecular plane than in the region defined by the π bond. A planar structure with a tilt of the argon atom toward this region of electron deficiency leads to a minimum in the exchange repulsion and consequently a stabilization of the T-shaped structure. The potential energy surface of the complex suggests that H_2CO undergoes an internal rotation with a barrier estimated to be 32 cm^{-1} (*4*). The *ab initio* calculations are in agreement with the microwave study of H_2CO–Ar that determined the effective structure to be T-shaped and probably planar (*3*). Two sets of microwave transitions were observed and assigned to internal rotor states which arise from hindered internal rotation about the C=O axis of formaldehyde (*3*).

Formaldehyde and ketene are the simplest members of the aldehyde and cumulene systems, respectively. As for H_2CO–Ar, internal rotation of the hydrogen atoms about the C=C=O axis of ketene should lead to the observation of two internal rotor states for H_2CCO–Ar. However, ketene has mutually orthogonal C=C and C=O π orbitals which may complicate the binding of the argon to ketene. In the present work, pulsed-nozzle Fourier–transform microwave spectroscopy is used to investigate the rotational spectra of H_2CCO–Ar, $H_2{}^{13}CCO$–Ar, $H_2C^{13}CO$–Ar, HDCCO–Ar, and D_2CCO–Ar. An effective structure is derived from the spectral data, evidence is presented for hindered internal rotation of ketene and the results are compared to those for H_2CO–Ar.

II. EXPERIMENTAL

Some of the rotational transitions of H_2CCO–Ar and D_2CCO–Ar were first observed at the National Institute of Standards and Technology during searches for the microwave spectra of H_2CCO–C_2H_2 and H_2CCO–C_2H_4 van der Waals complexes (*1, 2*). All spectral data reported in this paper were obtained at Rensselaer with a Fourier transform microwave spectrometer described in the literature (*5*). Pressurized tanks of 1% ketene in argon were used with pulsed solenoid valves to deliver gas pulses into the cavity of the spectrometer. The spectral lines assigned to argon–ketene isotopomers disappeared when neon was substituted for argon.

The most intense free induction decay signals of H_2CCO–Ar from a single gas pulse into the cavity were observed to have a signal to noise ratio of 150 to 1. Linewidths of 7 kHz were typically observed for H_2CCO–Ar when the gas pulses originated from a solenoid valve located in the cavity mirror (*6*). It

0022-2852/01 $35.00

is estimated that the center frequencies of the least intense transitions have a measurement precision of 2 kHz. Stark effects of the rotational transitions were used to obtain the spectral assignments and to measure the electric dipole moment of H_2CCO–Ar as described previously (*7*). The plate separation was determined by calibration using the $J = 1$–0 transition of OCS and its measured electric dipole moment of $2.38562(10)\times10^{-30}$ C m (0.71519(3) D) (*8*). Type *A* expanded uncertainties given here and throughout the text have a coverage factor of $k = 1$ (i.e., one standard deviation).

H_2CCO and D_2CCO were prepared by vacuum pyrolysis of acetic anhydride and deuterated acetic anhydride (99+ atom% deuterium), respectively, at 475°C (*9, 10*). The crude product was purified by vacuum distillation through a −78°C trap and collected at −195°C. There was sufficient enrichment of HDCCO in the D_2CCO sample to readily assign the spectrum of HDCCO–Ar.

III. SPECTRAL ANALYSIS

A planar, T-shaped configuration shown in Fig. 1 with $R_{cm} = 3.6$ Å and $\theta_{cm} = 90°$ was used to model the rotational spectrum of H_2CCO–Ar. This structure predicted the complex would have a number of intense low-J, *b*-type, *R* and *Q* rotational lines in the region 7–20 GHz. A spectrum consistent with the T-shaped model was observed and an assignment of the 1_{11}–0_{00}, 1_{10}–1_{01}, 2_{12}–1_{01}, and 3_{13}–2_{02} transitions was obtained employing Stark effects. The measured frequencies of these lines determined preliminary values of the rotational constants. These constants predicted the frequencies of additional *b*-type and much less intense *a*-type transitions that were measured to refine the spectral fit. Two lines were found for each rotational transition, and they were sorted into two sets by noting the 3/1 relative intensity of each pair. Table 1 lists the transition assignments and measured line frequencies of the two sets. The less intense set is designated A_1 and the more intense set is designated A_2. These two sets of lines arise from exchange of the hydrogen nuclei due to internal rotation of ketene. The A_1 state is the ground state and has an observed nuclear spin weight of 1, while a nuclear spin weight of 3 is found for the A_2 state. Both states were fit to an asymmetric top Watson Hamiltonian in the I^r representation and *A*-reduced form (*11*). Table 1 lists the residuals from the least-squares fits. In order to fit the line frequencies of both states to the estimated measurement uncertainty of 2 kHz, it was necessary to include the sextic centrifugal distortion constant, h_κ, as well as the five quartic constants. The rotational constants, distortion constants and overall standard deviation of the fits are given in Table 3.

Isotopic shifts, obtained from differences in the observed and calculated (T-shaped model) frequencies of the normal

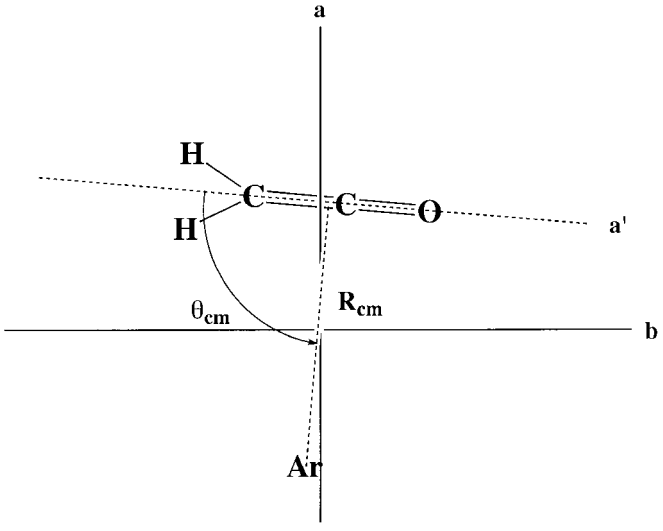

FIG. 1. A planar, T-shaped structure of H_2CCO–Ar showing the coordinates R_{cm} and θ_{cm} used to determine the geometry of the complex. The distance between the center of mass of H_2CCO and the argon atom is given by R_{cm} and θ_{cm} is the angle between the line connecting argon with the center of mass of H_2CCO and the a' axis of H_2CCO in the direction of the methylene carbon atom. *a* and *b* are the principal axes of H_2CCO–Ar and a' is the principal axis of H_2CCO which is coincident with the C=C=O axis.

TABLE 1
Observed and Calculated Transition Frequencies of H_2CCO

	State A_1, nuclear spin weight = 1		State A_2, nuclear spin weight =3	
$J'_{K_a',K_c'} \leftarrow J''_{K_a'',K_c''}$	ν_{obs}[a]	$\Delta\nu$[b]	ν_{obs}[a]	$\Delta\nu$[b]
$1_{10}\leftarrow1_{01}$	8 840.3399	3.3	8 810.3489	-0.8
$2_{11}\leftarrow2_{02}$	9 157.8488	2.0	9 106.2856	0.0
$3_{12}\leftarrow3_{03}$	9 649.4343	-0.1	9 563.5394	0.6
$5_{05}\leftarrow4_{14}$	10 220.4538	1.9	10 125.5621	-0.2
$4_{13}\leftarrow4_{04}$	10 333.0451	-1.6	10 197.7746	0.5
$3_{22}\leftarrow4_{13}$	10 427.0018	-0.5	10 505.4242	0.1
$3_{03}\leftarrow2_{02}$	10 539.5482	-1.2	10 518.2671	-1.8
$5_{15}\leftarrow4_{22}$	10 927.7452	2.3	10 736.8716	0.1
$5_{14}\leftarrow5_{05}$	11 231.5321	-2.4	11 029.0216	0.4
$1_{11}\leftarrow0_{00}$	12 054.6567	2.7	12 037.0272	-0.8
$6_{15}\leftarrow6_{06}$	12 371.0991	-1.6	12 080.4557	0.3
$7_{16}\leftarrow7_{07}$	13 778.7836	0.4	13 376.4083	-0.2
$3_{21}\leftarrow4_{14}$	13 569.5088	-0.2	13 434.3279	-0.3
$4_{14}\leftarrow3_{13}$	13 456.7191	-3.1	13 467.0947	0.0
$4_{04}\leftarrow3_{03}$	14 012.6614	-0.3	13 989.1421	0.0
$4_{23}\leftarrow3_{22}$	14 080.0133	0.0	14 049.4348	-0.1
$4_{22}\leftarrow3_{21}$	14 162.3436	-0.2	14 121.3775	-0.2
$6_{06}\leftarrow5_{15}$	14 268.3363	3.0	14 143.2442	0.7
$2_{21}\leftarrow3_{12}$	14 557.2739	-0.4	14 586.2900	0.8
$4_{13}\leftarrow3_{12}$	14 696.2717	-2.3	14 623.3772	-0.2
$2_{12}\leftarrow1_{01}$	15 267.5480	1.0	15 262.6159	-0.9
$2_{20}\leftarrow3_{13}$	16 427.1807	-1.1	16 330.0393	-0.8
$5_{15}\leftarrow4_{14}$	16 804.1070	-2.9	16 818.8350	0.6
$5_{05}\leftarrow4_{04}$	17 452.3133	0.3	17 430.5324	2.0
$5_{24}\leftarrow4_{23}$	17 587.1918	3.1	17 550.1573	-0.9
$5_{23}\leftarrow4_{22}$	17 750.7097	1.5	17 693.1351	-0.8
$3_{13}\leftarrow2_{02}$	18 327.3495	-0.5	18 345.2848	0.3
$7_{07}\leftarrow6_{16}$	18 334.6507	-1.7	18 184.9680	-1.1
$5_{14}\leftarrow4_{13}$	18 350.8016	0.7	18 261.7796	2.0

[a] The transition frequencies (MHz) have a combined standard uncertainty of 2 kHz.

[b] $\Delta\nu$ (kHz) are the observed minus calculated frequencies from the least-squares fit of ν_{obs} to the rotational and centrifugal distortion constants.

isotopomer, were used to predict the frequencies of rotational transitions of D_2CCO–Ar. Pairs of lines were found in the spectral regions calculated from the isotopic shifts. Lines of the ground state, designated A_1, were a factor of 2 more intense than those of the A_2 excited state. This 2/1 intensity ratio is expected from the nuclear spin weights by exchange of a pair of deuterium atoms due to internal rotation of D_2CCO. Many of the lines for the two internal rotor states exhibited resolved hyperfine splitting. Preliminary assignments and fits of the two states were obtained by using the measured frequency of the most intense hyperfine component for each line as the unsplit line frequency in the least squares fit to the Watson Hamiltonian described above for the normal isotopomer. In order to fit the transitions to the estimated measurement uncertainty of 2 kHz, it was necessary to analyze the deuterium hyperfine splitting observed for many of the transitions and obtain more accurate unsplit line frequencies. The internal motion of ketene makes the deuterium nuclei of D_2CCO–Ar equivalent. Hence, a coupling scheme applied to the H_2CCO–C_2D_2 complex (*1*) where tunneling leads to equivalent deuterium nuclei was used for D_2CCO–Ar. The two deuterium nuclei of nuclear spin 1 are coupled together, $I_1 + I_2 = I_D$, with $I_D = 0$, 1, and 2. I_D couples to the overall rotation of the complex, $J + I_D = F$. Since deuterium nuclei act as bosons upon exchange by the internal motion, the symmetric $I_D = 0, 2$ spin functions combine with the symmetric A_1 state and the antisymmetric $I_D = 1$ spin function with the antisymmetric A_2 state.

A first order nuclear electric quadrupole interaction of the two equivalent nuclei was used to iteratively fit the hyperfine components of the A_1 and A_2 states (*12*). Table 2 lists the measured hyperfine line frequencies, assignments and residuals from this least-squares fit. The unsplit line centers of the A_1 and A_2 states and the quadrupole coupling constants obtained from this fit are given in Table 3 and Table 4, respectively. An overall standard deviation of 1.2 kHz was found for the fit that is within the estimated measurement precision of 2 kHz for the measured hyperfine components. The unsplit line centers and a number of transitions with unresolved hyperfine components were fit separately for the A_1 and A_2 states to the Watson Hamiltonian used for the normal isotopomer as described above. Table 4 contains the spectral constants obtained from these fits for the two states.

Isotopic shifts from the normal isotopomer were used to predict the frequencies of rotational transitions of $H_2C^{13}CO$–Ar and $H_2{}^{13}CCO$–Ar. It was possible to observe and assign both of these isotopomers in natural abundance. Transitions were not intense enough to identify the Stark effects, which made the assignments difficult particularly with the presence of two states for each carbon-13 isotopomer. The less intense sets of lines were assigned to the A_1 states, as described above for the normal isotopomer. Tables 5 and 6 list the measured line frequencies, quantum assignments, and residuals from least-squares fits of the frequencies to the Hamiltonian used for the normal isotopomer described above. In these fits, Δ_K and δ_K were constrained to the values determined for the A_1 and A_2 states of the normal

TABLE 2
Observed and Calculated Hyperfine Transition Frequencies of D_2CCO–Ar

	State A_1 (I = 0,2)			State A_2 (I = 1)		
$J'_{K'_a,K'_c} \leftarrow J''_{K''_a,K''_c}$	F', I'←F'', I''	ν_{obs}[a]	$\Delta\nu$[b]	F', I'←F'', I''	ν_{obs}[a]	$\Delta\nu$[b]
3_{22}←4_{13}	3, 0←4, 0	7 357.0499	-0.6	2, 1←3, 1	7 453.1304	-0.8
	4, 2←5, 2	7 357.0636	0.6	4, 1←5, 1	7 453.1356	0.1
	5, 2←6, 2	7 357.0828	-0.4	3, 1←4, 1	7 453.1530	0.7
	3, 2←4, 2	7 357.0879	0.4			
	1, 2←2, 2	7 357.0917	-0.1			
1_{10}←1_{01}	3, 2←2, 2	7 691.0525	0.9	1, 1←0, 1	7 684.0090	-1.4
	2, 2←3, 2	7 691.0609	1.4	0, 1←1, 1	7 684.0216	-1.9
	3, 2←3, 2	7 691.0913	-0.2	2, 1←2, 1	7 684.0284	-0.5
	1, 2←1, 0	7 691.0949	-0.2	2, 1←1, 1	7 684.0570	1.5
	2, 2←1, 2	7 691.1075	-1.1	1, 1←1, 1	7 684.0790	2.2
	1, 0←1, 2	7 691.1110	-0.8			
2_{11}←2_{02}	4, 2←4, 2	8 024.1952	0.0	1, 1←1, 1	8 003.8047	-3.6
				3, 1←3, 1	8 003.8223	1.1
				2, 1←2, 1	8 003.8468	2.4
4_{22}←5_{15}	4, 0←5, 0	8 176.6524	1.4			
	5, 2←6, 2	8 176.6729	0.0			
	6, 2←7, 2	8 176.7025	-1.4			
3_{12}←3_{03}	4, 2←4, 2	8 543.0603	0.5	2, 1←2, 1	8 501.2425	-1.2
	5, 2←5, 2	8 543.0808	-0.4	4, 1←4, 1	8 501.2498	0.1
	3, 2←3, 2	8 543.0872	-0.1	3, 1←3, 1	8 501.2680	1.2
4_{13}←4_{04}	4, 0←4, 0	9 270.0571	0.6	3, 1←3, 1	9 196.9559	-1.2
	5, 2←5, 2	9 270.0682	0.5	5, 1←5, 1	9 196.9611	0.2
	3, 2←3, 2	9 270.0778	-1.5	4, 1←4, 1	9 196.9770	1.0
	6, 2←6, 2	9 270.0853	-0.4			
	4, 2←4, 2	9 270.0899	0.3			
	2, 2←2, 2	9 270.0571	0.4			
3_{03}←2_{02}	5, 2←4, 2	10 188.0688	-0.6			
	3, 2←2, 2	10 188.0757	0.5			
	3, 0←2, 0	10 188.0757	0.2			
5_{14}←5_{05}	5, 0←5, 0	10 233.1430	0.4	4, 1←4, 1	10 116.8972	-1.0
	6, 2←6, 2	10 233.1541	0.1	6, 1←6, 1	10 116.9010	-0.1
	4, 2←4, 2	10 233.1626	-0.2	5, 1←5, 1	10 116.9167	1.2
	7, 2←7, 2	10 233.1705	-0.3			
3_{21}←4_{14}	3, 0←4, 0	10 642.2852	1.3	2, 1←3, 1	10 607.4358	-3.3
	4, 2←5, 2	10 642.3107	0.1	4, 1←5, 1	10 607.4484	-0.1
	2, 2←3, 2	10 642.3389	0.3	3, 1←4, 1	10 607.4879	3.4
	5, 2←6, 2	10 642.3527	-1.1			
	3, 2←4, 2	10 642.3626	-0.6			
1_{11}←0_{00}	2, 2←2, 2	10 777.7127	0.2	0, 1←1, 1	10 774.4095	-0.8
	1, 0←2, 2	10 777.7127	-0.6	2, 1←1, 1	10 774.4182	0.0
	1, 0←0, 0	10 777.7127	-0.6	1, 1←1, 1	10 774.4242	0.8
	3, 2←2, 2	10 777.7204	0.0			
	1, 2←0, 0	10 777.7305	0.5			
	1, 2←2, 2	10 777.7305	0.5			
5_{05}←4_{14}	6, 2←5, 2	10 803.6455	0.3			
	5, 0←4, 0	10 803.6455	-0.1			
	4, 2←3, 2	10 803.6520	0.4			
	3, 2←2, 2	10 803.6524	-0.6			
2_{21}←3_{12}	2, 0←3, 0	11 394.3752	1.6	1, 1←2, 1	11 456.9101	-1.2
	3, 2←4, 2	11 394.3970	1.5	3, 1←4, 1	11 456.9316	-0.2
	4, 2←5, 2	11 394.4484	-1.7	2, 1←3, 1	11 456.9749	1.4
	2, 2←3, 2	11 394.4698	-1.4			
4_{14}←3_{13}	6, 2←5, 2	12 969.3889	0.0			
	5, 2←4, 2	12 969.3916	-0.4			
	2, 2←1, 2	12 969.3916	-1.1			
	3, 2←2, 2	12 969.3984	0.7			
	4, 0←3, 0	12 969.3984	0.7			

[a] The hyperfine transition frequencies (MHz) have a combined standard uncertainty of 2 kHz.

[b] $\Delta\nu$ (kHz) is the observed minus calculated hyperfine frequencies from the deuterium quadrupole fit.

TABLE 2—*Continued*

	State A_1 (I = 0,2)			State A_2 (I = 1)		
$J'_{K'_a,K'_c} \leftarrow J''_{K''_a,K''_c}$	F', I'←F'', I''	ν_{obs}[a]	$\Delta\nu$[b]	F', I'←F'', I''	ν_{obs}a	$\Delta\nu$[b]
$2_{20}\leftarrow3_{13}$	2, 0←3, 0	13 345.9028	2.2	1, 1←2, 1	13 331.3863	-1.8
	3, 2←4, 2	13 345.9363	1.9	3, 1←4, 1	13 331.4137	-1.3
	4, 2←5, 2	13 346.0100	-1.8	2, 1←3, 1	13 331.4782	3.2
	2, 2←3, 2	13 346.0373	-2.2			
$2_{12}\leftarrow1_{01}$	3, 2←2, 2	13 863.1891	-0.9	3, 1←2, 1	13 863.8336	-1.0
	4, 2←3, 2	13 863.1987	-0.6	2, 1←1, 1	13 863.8381	-0.3
	2, 0←1, 0	13 863.2043	-0.3	1, 1←1, 1	13 863.8752	1.3
	3, 2←3, 2	13 863.2303	0.5			
	2, 2←1, 2	13 863.2366	1.3			
$4_{13}\leftarrow3_{12}$	6, 2←5, 2	14 261.6267	-0.1			
	4, 2←3, 2	14 261.6267	-0.5			
	2, 2←1, 2	14 261.6267	-0.8			
	5, 2←4, 2	14 261.6324	2.1			
	3, 2←2, 2	14 261.6324	1.1			
	4, 0←3, 0	14 261.6324	-1.8			
$6_{06}\leftarrow5_{15}$	6, 0←5, 0	14 710.0629	-0.1			
	7, 2←6, 2	14 710.0629	-1.1			
	8, 2←7, 2	14 710.0694	1.4			
	5, 2←4, 2	14 710.0694	0.1			
	6, 2←5, 2	14 710.0694	-0.3			
$3_{13}\leftarrow2_{02}$	5, 2←4, 2	16 789.9762	-0.4			
	4, 2←3, 2	16 789.9762	-1.0			
	3, 2←2, 2	16 789.9839	1.7			
	3, 0←2, 0	16 789.9839	-0.3			

TABLE 3
Unsplit Rotational Transitions of D_2CCO–Ar

	State A_1, nuclear spin weight = 2		State A_2, nuclear spin weight =1	
$J'_{K'_a,K'_c} \leftarrow J''_{K''_a,K''_c}$	ν_0[a]	$\Delta\nu_0$[b]	ν_0[a]	$\Delta\nu_0$[b]
$3_{22}\leftarrow4_{13}$	7 357.0742	0.5	7 453.1400	0.2
$1_{10}\leftarrow1_{01}$	7 691.0755	0.8	7 684.0369	0.6
$2_{11}\leftarrow2_{02}$	8 024.1849	0.2	8 003.8263	-1.1
$4_{22}\leftarrow5_{15}$	8 176.6888	0.3		
$3_{12}\leftarrow3_{03}$	8 543.0726	0.3	8 501.2540	0.5
$4_{13}\leftarrow4_{04}$	9 270.0777	-0.2	9 196.9649	0.3
$3_{03}\leftarrow2_{02}$	10 188.0718	-1.7	10 164.3088[c]	-2.3
$5_{14}\leftarrow5_{05}$	10 233.1628	-0.1	10 116.9051	-0.5
$3_{21}\leftarrow4_{14}$	10 642.3347	-0.1	10 607.4581	0.3
$1_{11}\leftarrow0_{00}$	10 777.7186	0.2	10 774.4190	-0.5
$5_{05}\leftarrow4_{14}$	10 803.6483	0.1	10 720.3394[c]	0.8
$2_{21}\leftarrow3_{12}$	11 394.4308	0.1	11 456.9414	0.0
$4_{14}\leftarrow3_{13}$	12 969.3920	-0.8	12 960.7736[c]	-1.1
$2_{20}\leftarrow3_{13}$	13 345.9834	-0.8	13 331.4292	-0.5
$4_{04}\leftarrow3_{03}$	13 534.6253[c]	1.3	13 506.5753[c]	-1.1
$2_{12}\leftarrow1_{01}$	13 863.2006	-0.1	13 863.8340	0.9
$4_{13}\leftarrow3_{12}$	14 261.6291	-0.5	14 202.2881[c]	0.6
$6_{06}\leftarrow5_{15}$	14 710.0670	1.6	14 608.6336[c]	1.2
$5_{15}\leftarrow4_{14}$	16 191.7626[c]	-0.2	16 182.2881[c]	-0.2
$3_{13}\leftarrow2_{02}$	16 789.9794	-0.8	16 800.6742[c]	0.5
$5_{05}\leftarrow4_{04}$	16 840.3250[c]	1.4	16 810.9011[c]	1.6
$5_{14}\leftarrow4_{13}$	17 803.4090[c]	0.3		
$7_{07}\leftarrow6_{16}$	18 612.9491[c]	-1.2	18 498.3626[c]	-1.1

[a] ν_0 (MHz) is the unsplit center frequency obtained from the deutrium quadrupole fit listed in Table 2.

[b] $\Delta\nu_0$ (kHz) is the ν_0 minus calculated frequencies from the least-squares fit of ν_0 to the rotational and centrifugal distortion constants.

[c] No resolved hyperfine transitions are observed; transition frequency used only for the unsplit line fit.

TABLE 4
Spectroscopic Constants of H_2CCO–Ar and D_2COO–Ar

	H_2CCO-Ar		D_2CCO-Ar	
	State A_1	State A_2	State A_1	State A_2
A(MHz)	10 447.9248(10)[a]	10 423.9698(4)	9 234.7208(6)	9 229.4837(7)
B(MHz)	1 918.0138(16)	1 903.1868(8)	1 867.3508(21)	1 856.4206(38)
C(MHz)	1 606.7642(15)	1 613.0940(7)	1 543.0081(20)	1 544.9605(36)
$\Delta(u\cdot Å^2)$	2.67013	-0.72805	2.16288	0.12447
Δ_J(kHz)	16.0856(70)	15.7691(31)	14.191(10)	14.027(19)
Δ_{JK}(kHz)	274.779(64)	192.798(28)	219.651(78)	172.60(11)
Δ_K(kHz)	-152.24(23)	-136.16(10)	-143.44(11)	-117.40(16)
δ_J(kHz)	2.5313(18)	2.50745(82)	2.4112(18)	2.3974(29)
δ_K(kHz)	209.85(82)	134.88(39)	167.1(10)	125.7(18)
h_K(kHz)	1.562(64)	1.593(30)	0.900(41)	0.951(59)
σ(kHz)[b]	2.2	1.0	1.0	1.2
eQq_{bb}(kHz)			-17.4(5)	
eQq_{cc}(kHz)			-71.1(6)	

[a] Quantities in parentheses are Type A expanded uncertainties with a coverage factor $k = 1$, i.e., $\sigma = 1$.

[b] σ is the overall standard deviation of the least-squares fit.

isotopomer and h_K was not included in the Hamiltonian. It was not possible to measure the frequencies of sufficient lines to determine Δ_K, δ_K, and h_K. The spectral constants obtained from these fits are listed in Table 8.

The assignment of the rotational spectrum of HDCCO–Ar was aided by a heavy atom structure derived from moment of inertia fits of the normal and carbon-13 isotopomers as described in Section V. Both a nonplanar structure, where the hydrogen atoms are located orthogonal to the heavy atom plane (I in Fig. 2), and a planar structure (II in Fig. 2) were considered for the spectral predictions. In the latter case, the internal rotation is quenched, but substitution of the deuterium in ketene leads to two structurally distinct configurations with different rotational constants.

TABLE 5
Observed and Calculated Transition Frequencies of $H_2C^{13}CO$–Ar

	State A_1, nuclear spin weight = 1		State A_2, nuclear spin weight =3	
$J'_{K'_a,K'_c} \leftarrow J''_{K''_a,K''_c}$	ν_{obs}	$\Delta\nu$[a]	ν_{obs}	$\Delta\nu$[a]
$1_{10}\leftarrow1_{01}$	8 854.8855	-1.2	8 825.2137	-3.8
$2_{11}\leftarrow2_{02}$	9 165.7498	-1.5	9 114.9742	-1.9
$3_{12}\leftarrow3_{03}$	9 646.7249	-0.3	9 562.4011	0.2
$5_{05}\leftarrow4_{14}$	10 000.3113	-0.5	9 907.7507	-1.0
$4_{13}\leftarrow4_{04}$	10 315.0147	0.6	10 182.5085	1.0
$5_{14}\leftarrow5_{05}$	11 192.5630	0.9	10 994.5259	1.0
$1_{11}\leftarrow0_{00}$	12 039.0993	1.2	12 021.6956	3.2
$6_{15}\leftarrow6_{06}$	12 304.6201	-0.6	12 020.7692	-0.8
$6_{06}\leftarrow5_{15}$	14 006.3481	-0.1	13 883.7411	-0.2
$2_{12}\leftarrow1_{01}$	15 221.9142	1.8	15 217.1019	2.6
$7_{07}\leftarrow6_{16}$	18 032.9687	0.3	17 885.5477	0.6
$3_{13}\leftarrow2_{02}$	18 254.6817	-1.3	18 272.4300	-2.2

[a] The transition frequencies (MHz) have a combined standard uncertainty of 2 kHz.

[b] $\Delta\nu$ (kHz) are the observed minus calculated frequencies from the least-squares fit of ν_{obs} to the rotational and centrifugal distortion constants.

TABLE 6
Observed and Calculated Transition Frequencies of $H_2C^{13}CCO$–Ar

	State A_1, nuclear spin weight = 1		State A_2, nuclear spin weight = 3	
$J'_{K_a',K_c'} \leftarrow J''_{K_a'',K_c''}$	ν_{obs}	$\Delta\nu$[a]	ν_{obs}	$\Delta\nu$[a]
$1_{10}\leftarrow1_{01}$	8 547.9801	-1.2	8 513.2933	1.0
$2_{11}\leftarrow2_{02}$	8 866.1861	-1.0	8 811.0604	-2.5
$3_{12}\leftarrow3_{03}$	9 359.3890	-0.4	9 271.6858	-0.7
$4_{13}\leftarrow4_{04}$	10 046.1809	0.1	9 911.5320	0.4
$5_{05}\leftarrow4_{14}$	10 255.3109	-1.0	10 177.9415	-0.5
$5_{14}\leftarrow5_{05}$	10 950.1688	1.3	10 751.4701	1.6
$1_{11}\leftarrow0_{00}$	11 712.0348	0.6	11 690.0583	-0.2
$6_{15}\leftarrow6_{06}$	12 098.2636	-0.7	11 815.5064	-0.8
$6_{06}\leftarrow5_{15}$	14 245.3485	0.7	14 141.2641	0.1
$2_{12}\leftarrow1_{01}$	14 874.7267	2.3	14 865.7857	2.3
$3_{13}\leftarrow2_{02}$	17 884.3276	-1.4	17 898.0307	-1.2
$7_{07}\leftarrow6_{16}$	18 249.8052	0.0	18 124.6364	0.2

[a] The transition frequencies (MHz) have a combined standard uncertainty of 2 kHz.

[b] $\Delta\nu$ (kHz) are the observed minus calculated frequencies from the least-squares fit of ν_{obs} to the rotational and centrifugal distortion constants.

One form contains the deuterium in the position closest to the argon atom (Ia in Fig. 2), and the second has the deuterium located on the opposite side of the C=C=O axis away from the argon atom (Ib in Fig. 2). Since the zero point energies of the two forms are different, the higher energy form may not be populated in the cold gas pulse and consequently its spectrum may not be seen. A number of examples of this zero point energy effect are known and have been discussed in the literature for complexes (*13*) and monomers (*5*). Internal rotation of ketene in the nonplanar configuration exchanges a hydrogen atom for

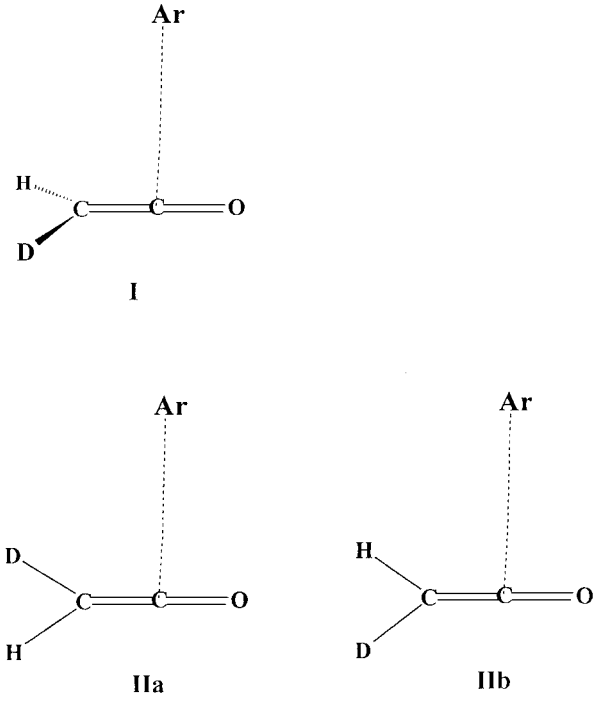

FIG. 2. Nonplanar, I, and planar, II, geometries of HDCCO–Ar. IIa and IIb are structurally different isotopomers and correspond to the deuterium atom located either adjacent (IIa) or opposite the argon atom in the complex.

TABLE 7
Rotational Transitions of HDCCO–Ar

$J'_{K_a',K_c'} \leftarrow J''_{K_a'',K_c''}$	F'←F''	ν_{obs}[a]	$\Delta\nu$[b]	ν_0[c]	$\Delta\nu_0$[d]
$1_{10}\leftarrow1_{01}$				8 221.1558	-5.2
	2←2	8 221.1631	0.4		
	1←0	8 221.1793	-0.6		
$2_{11}\leftarrow2_{02}$				8 547.0936	14.4
	2←2	8 547.0782	-0.3		
	3←3	8 547.0967	-1.2		
	1←1	8 547.1094	0.7		
$3_{12}\leftarrow3_{03}$				9 053.1802	19.3
	3←3	9 053.1693	-0.4		
	4←4	9 053.1836	-0.1		
	2←2	9 053.1888	0.2		
$4_{13}\leftarrow4_{04}$				9 759.4405	1.7
	4←4	9 759.4315	-0.2		
	5←5	9 759.4437	0.0		
	3←3	9 759.4469	0.1		
$3_{03}\leftarrow2_{02}$				10 349.8511	-4.1
	4←3	10 540.8505	0.0		
$5_{05}\leftarrow4_{14}$				10 540.4204	2.3
	6←5	10 540.4204	0.0		
$5_{14}\leftarrow5_{05}$				10 691.1043	-25.0
	5←5	10 691.0958	-0.3		
	6←6	10 691.1077	0.3		
$1_{11}\leftarrow0_{00}$				11 365.8013	-18.2
	1←1	11 365.7963	-0.4		
	2←1	11 365.8022	0.0		
	0←1	11 365.8108	0.3		
$6_{15}\leftarrow6_{06}$				11 876.5292	9.9
	6←6	11 876.5197	-1.5		
	7←7	11 876.5339	1.5		
$2_{21}\leftarrow3_{12}$				12 846.7310	(147.3)[e]
	2←3	12 846.7007	1.2		
	3←4	12 846.7412	-1.4		
$4_{04}\leftarrow3_{03}$				13 753.9864	6.2
	5←4	13 753.9857	0.0		
$2_{12}\leftarrow1_{01}$				14 508.2229	-5.1
	3←2	14 508.2221	-0.4		
	1←0	14 508.2474	0.4		
$6_{06}\leftarrow5_{15}$				14 513.4320	9.9
	7←6	14 513.4322	-0.1		
$2_{20}\leftarrow3_{13}$				14 765.2140	(-276.4)[e]
	2←3	14 765.1761	-1.7		
	3←4	14 765.2246	1.7		
$5_{05}\leftarrow4_{04}$				17 120.1225	-7.1
	6←5	17 120.1225	0.6		
$3_{13}\leftarrow2_{02}$				17 493.5197	11.4
	4←3	17 493.5194	0.7		
$7_{07}\leftarrow6_{16}$				18 492.3390	-4.4
	8←7	18 492.3394	0.0		

[a] The hyperfine transition frequencies (MHz) have a combined standard uncertainty of 2 kHz.

[b] $\Delta\nu$ (kHz) is the observed minus calculated hyperfine frequencies from the deuterium quadrupole fit.

[c] ν_0 (MHz) is the unsplit center frequency obtained from the deuterium quadrupole fit.

[d] $\Delta\nu_0$ (kHz) is the ν_0 minus calculated frequencies from the least-squares fit of ν_0 to the rotational and centrifugal distortion constants.

[e] Not included in the least-squares fit.

TABLE 8
Spectroscopic Constants of $H_2C^{13}CO$–Ar, $H_2{}^{13}CCO$–Ar, and HDCCO–Ar

	$H_2C^{13}CO$-Ar		$H_2{}^{13}CCO$-Ar		HDCCO-Ar
	State A_1	State A_2	State A_1	State A_2	
A(MHz)	10 447.4101(10)[a]	10 423.7274(19)	10 130.4103(10)	1 0101.9370(12)	9 794.462(11)
B(MHz)	1 896.6464(3)	1 882.2011(5)	1 893.2223(3)	1 879.7003(3)	1 890.951(4)
C(MHz)	1 591.7077(2)	1 597.9886(4)	1 581.6281(2)	1 588.1337(3)	1 572.311(6)
Δ(u·Å^2)	2.67453	-0.72833	2.70236	-0.66745	2.56408
Δ_J(kHz)	15.8461(44)	15.5144(85)	15.6905(45)	15.3441(54)	22.350(92)
Δ_{JK}(kHz)	269.099(99)	188.72(18)	261.69(10)	183.44(12)	463.48()82
Δ_K(kHz)	-152.2[b]	-136[b]	-152.2[b]	-136[b]	
δ_J(kHz)	2.4837(24)	2.4644(45)	2.5237(25)	2.5282(29)	5.844(43)
δ_K(kHz)	209.85[b]	135[b]	209.8[b]	135[b]	
h_K(kHz)					-19.9(18)
σ(kHz)[c]	1.4	2.7	1.5	1.7	16.0
eQq_{bb}(kHz)					-18.4(8)
eQq_{cc}(kHz)					-59.7(9)

[a] Quantities in parentheses are Type A expanded uncertainties with a coverage factor $k = 1$, i.e., $\sigma = 1$.
[b] Constrained to this value in the least-squares fit.
[c] σ is the overall standard deviation of the least-squares fit.

a deuterium atom, which gives two equivalent but nonsuperimposable frameworks. Hence, two states are expected with equal spin weights.

Spectral searches over the frequency ranges predicted for the two forms, I and II(a,b), revealed the presence of only one set of rotational transitions. The transitions exhibited hyperfine splitting due to the presence of one deuterium quadrupolar nucleus. Table 8 contains the measured line frequencies, spectral assignments and the residuals from an iterative fit of the hyperfine frequencies using a first order nuclear electric quadrupole interaction (*14*). This fit gave the unsplit line centers, also listed in Table 7 and the deuterium quadrupole coupling constants, given in Table 8, with an overall standard deviation of 0.2 kHz. The results of the best fit of the unsplit line centers to the rotational constants and the distortion constants, Δ_J, Δ_{JK}, δ_J, and h_K, are listed in Tables 7 and 8. The overall standard deviation of 16.0 kHz obtained for this fit is at least a factor of 8 higher than analogous fits for the same transitions of the A_1 or A_2 states of the H_2CCO–Ar and D_2CCO–Ar isotopomers using the same Hamiltonian. In order to fit the 2_{21}–3_{12} and 2_{20}–3_{13} P-branch transitions of HDCCO–Ar, it is necessary to also include Δ_K or δ_K. This reduces the overall standard deviation by a factor of 2 but introduces high correlation between a few of the spectral constants. While the effect is not large, it suggests small perturbations of rotational states for this isotopomer not present in H_2CCO–Ar and D_2CCO–Ar. These perturbations are presumably due to interactions between the two isomeric states, made possible by the small energy separations.

IV. ELECTRIC DIPOLE MOMENT

Electric dipole moments of the A_1 and A_2 states of H_2CCO–Ar were determined by measuring frequency shifts of Stark transitions in the presence of applied DC electric fields oriented parallel to the microwave electric field (*7*). Electric fields up to 290 V/cm were employed and frequency shifts as large as 1.1 MHz were observed in the measurements of the following seven Stark components: 1_{11}–0_{00} $M_J = 0$, 1_{10}–1_{01} $M_J = 1$, 2_{12}–1_{01} $M_J = 0$ and 1, the 2_{11}–2_{02} $M_J = 2$, and 3_{12}–3_{03} $M_J = 2$ and 3. All components exhibited second order Stark behavior. A least squares fit of 38 measurements of the A_1 state to μ_a^2 and μ_b^2 gave the results $\mu_a = 0.417(10)\times10^{-30}$ C m (0.125(3) D) and $\mu_b = 4.566(7)\times10^{-30}$ C m (1.369(2) D). When the data are fit to μ_a^2, μ_b^2, and μ_c^2, μ_a and μ_b do not change significantly and μ_c is found to be zero to within one standard deviation. An analogous least squares fit of 51 measurements of the A_2 state to μ_a^2, μ_b^2, and μ_c^2 found μ_c to be zero. A fit of the data to μ_a^2 and μ_b^2 gave $\mu_a = 0.290(3)\times10^{-30}$ C m (0.087(1) D) and $\mu_b = 4.570(13)\times10^{-30}$ C m (1.370(4) D). Hence, the dipole moment components are nearly the same for the A_1 and A_2 states.

V. STRUCTURE

A heavy atom structure of H_2CCO–Ar can be viewed as a ball and stick where argon is the ball and the linear C=C=O backbone of ketene is the stick. The spectral data presented in Sections III and IV show that argon is approximately perpendicular to the C=C=O axis (Fig. 1). For this T-shaped geometry the b inertial axis of the complex is aligned close to parallel to the a inertial axis of ketene (designated a′ in Fig. 1), so the A rotational constant of Ar-ketene is close to the value reported for the B rotational constant of ketene. For H_2CCO–Ar, $A = 10\,477.9248$ MHz compares closely to $B = 10\,293.3175$ MHz for H_2CCO (*15*). The other four isotopomers of H_2CCO–Ar have A rotational constants that are close to the values of the B rotational constants of the corresponding ketene isotopomer (*15*).

The dipole moment measurement of H_2CCO–Ar also is consistent with a T-shaped complex. H_2CCO has a measured dipole moment (*16*) of 1.42215 D which is close to the measured value of $\mu_b = 1.369(2)$ D in the complex.

The inertial defects of the ground states for the normal and carbon-13 isotopomers listed in Tables 4 and 8 are large and have nearly the same values ($\Delta = I_c - I_b - I_a = 2.67013$ uÅ^2 for H_2CCO–Ar) as expected for substitution of the carbon atoms in a plane (*14*). Similar large positive inertial defects have been found for a number of T-shaped, ball and stick argon complexes including Ar–ClCN (*17*), Ar–OCS (*18*), and Ar–CO_2 (*19*). In these cases, the complexes are planar and zero-point motions of the van der Waals vibrations give rise to the large positive inertial defects. Although the large positive inertial defect observed for H_2CCO–Ar is consistent with a planar structure, internal rotation of ketene in the complex makes it difficult to determine the equilibrium positions of the hydrogen atoms. The observation of only one state for HDCCO–Ar suggests that the hydrogen atoms are also located in the heavy atom plane for the equilibrium configuration. However, there are significant zero point vibrational effects observed for HDCCO–Ar and D_2CCO–Ar, where the inertial defects decrease by 0.10605 and 0.50725 uÅ^2, respectively.

For a planar rigid complex where there is no change in the ketene geometry upon complexation, the two parameters, R_{cm} and θ_{cm}, determine the structure. As shown in Fig. 1, R_{cm} is the distance between the center of mass of ketene and the argon atom and θ_{cm} is the angle between R_{cm} and the a' axis of H_2CCO in the direction of the methylene carbon atom. These parameters can be calculated from the moment of inertia equations

$$I_{aa}(\mathrm{H_2CCO\text{–}Ar}) = I_{bb}(\mathrm{H_2CCO})\sin^2\theta_{cm} \quad [1]$$

$$I_{bb}(\mathrm{H_2CCO\text{–}Ar}) = m_r R_{cm}^2 + I_{aa}(\mathrm{H_2CCO})\cos^2\theta_{cm} \quad [2]$$

$$I_{cc}(\mathrm{H_2CCO\text{–}Ar}) = m_r R_{cm}^2 + I_{cc}(\mathrm{H_2CCO}). \quad [3]$$

In these equations m_r is the pseudodiatomic reduced mass of the complex and I_{ii} are the effective moments of inertia of ketene (*15*) and of Ar–ketene. Table 9 lists the values of R_{cm} and θ_{cm} calculated from these equations for all five isotopomers. R_{cm} is obtained from Eq. [2] using the value of θ_{cm} calculated from Eq. [1] and directly from Eq. [3], There is good agreement between the two values of R_{cm} for all the isotopomers. D_2CCO–Ar exhibits the largest difference, 0.011 Å, which is close to the uncertainty of 0.01 Å estimated for other ball and stick complexes when the moments of inertia are not corrected for vibrational effects (*17, 18*). I_{bb} (Ar–ketene) contains the largest vibrational contributions, including the hydrogen internal rotation, so it is best to use Eq. [1] to calculate θ_{cm}, where the uncertainty due to neglect of the vibrational effects is estimated to be 1°(*17, 18*). The variation in θ_{cm} calculated from Eq. [1] is 0.4° for the five isotopomers listed in Table 9. Equation [2] gives very different results from Eq. [1] for HDCCO–Ar and D_2CCO–Ar and leads to negative values of $\cos^2\theta_{cm}$ for H_2CCO–Ar and $H_2C^{13}CO$–Ar.

TABLE 9
Structural Parameters of Argon–Ketene Calculated from Effective Moments of Inertia

Isotopomer	R_{cm} (Å)		θ_{cm} (°)	
	Eq.[1], Eq.[2][a]	Eq.[3]	Eq.[1]	Eq.[2], Eq.[3]
H_2CCO-Ar	3.586	3.587	83.0	-[b]
$H_2{}^{13}CCO$-Ar	3.585	3.589	82.6	84.8
$H_2C^{13}CO$-Ar	3.586	3.587	83.0	-[b]
HDCCO-Ar	3.590	3.585	82.9	53.5
D_2CCO-Ar	3.591	3.580	83.6	38.3

[a] Equations [1], [2] and [3] are given in the text; the values of R_{cm} and θ_{cm} are calculated from the designated equations.
[b] Equation [2] gives a negative value for $\cos^2\theta_{cm}$.

Equation [1] does not distinguish $\theta_{cm} = 83°$ from the supplementary value of 97°. The agreement between the experimental rotational constants of $H_2{}^{13}CCO$–Ar and those calculated from $R_{cm} = 3.586$ Å and $\theta_{cm} = 97.0°$ (obtained from Eq. [3] and Eq. [1] for H_2CCO–Ar) is much better than with the calculated rotational constants of $H_2{}^{13}CCO$–Ar using $R_{cm} = 3.586$ Å and $\theta_{cm} = 83.0°$. These results suggest that argon is tilted by about 7° toward the carbonyl carbon atom of ketene. Least squares fits of the moments of inertia of H_2CCO–Ar, $H_2C^{13}CO$–Ar, and $H_2{}^{13}CCO$–Ar to R_{cm} and θ_{cm} suggest the same tilt angle. In these fits the structure will converge to either value of θ_{cm}, depending upon whether the initial value of the angle is greater than or less than 90°. However, the overall standard deviation of the fit is much smaller for $\theta_{cm} = 97°$. For example, a fit of I_{aa} and I_{cc} of H_2CCO–Ar, $H_2C^{13}CO$–Ar, and $H_2{}^{13}CCO$–Ar beginning at $\theta_{cm} \geq 90°$ converges to $R_{cm} = 3.5868(3)$ Å and $\theta_{cm} = 96.4°(2)$ with an overall standard deviation of $\sigma = 0.072$ uÅ^2. An analogous fit starting at $\theta_{cm} < 90°$ converges to $R_{cm} = 3.589(1)$ Å and $\theta_{cm} = 83.5°$ (*9*) with an overall standard deviation of $\sigma = 0.36$ uÅ^2. In these fits the hydrogen atoms were constrained to the heavy atom plane by setting φ_{cm} to zero and the geometry of ketene was fixed at the reported r_0 values (*15*), $R_{CO} = 1.1626$ Å, $R_{CC} = 1.3147$ Å, $R_{CH} = 1.0905$ Å, and $\angle(\mathrm{HCH}) = 123.46°$. In order to test the planarity of the hydrogen atoms, I_{aa} and I_{cc} of H_2CCO–Ar, $H_2C^{13}CO$–Ar, and $H_2{}^{13}CCO$–Ar were fit to R_{cm} and θ_{cm}, constraining φ_{cm} to values from 0° to 90°. The standard deviation of these fits increased from $\sigma = 0.072$ uÅ^2 at $\varphi_{cm} = 0°$ to $\sigma = 0.098$ uÅ^2 for $\varphi_{cm} = 90°$. Hence, the effective moments of inertia of the three isotopomers are most consistent with a planar structure.

A comparison of the carbonyl and methylene carbon coordinates calculated by the substitution method (*14*) with those determined from the least squares fits discussed above also suggest the argon atom is tilted toward the carbonyl carbon of ketene in the complex. Rudolph's equations for a planar species using the measured moments of inertia of H_2CCO–Ar, $H_2C^{13}CO$–Ar,

and $H_2{}^{13}CCO$–Ar (*14*) gave the following absolute values of the atomic coordinates (in Å): carbonyl carbon, $|a| = 1.7312$, $|b| = 0.0494$; and methylene carbon, $|a| = 1.8679$, $|b| = 1.2533$. These substitution coordinates may be compared with the carbon coordinates determined from the least squares fits of the moments of inertia to R_{cm} and θ_{cm}. The fit with $\theta_{cm} = 96.4^\circ$ found the carbonyl carbon coordinates (in Å) of $a = 1.745$, $b = 0.0625$, and the methylene carbon coordinates of $a = 1.923$, $b = -1.240$. The corresponding fit with $\theta_{cm} = 83.5^\circ$ gave carbonyl carbon coordinates (in Å) of $a = 1.752$, $b = -0.0219$, and methylene carbon coordinates of $a = 1.572$, $b = -1.324$. Better agreement is found between the substitution coordinates and the fit with $\theta_{cm} = 96.4^\circ$. This is particularly true for the methylene carbon *a* coordinate, which is most sensitive to the tilt of the argon atom with respect to ketene. The sign assignment for the small carbonyl carbon *b* coordinate from the fit with $\theta_{cm} = 96.4^\circ$ gives a substitution carbon–carbon bond distance of 1.328(24) Å, while the opposite sign for this coordinate as determined from the fit with $\theta_{cm} = 83.5^\circ$ gives an unreasonable carbon–carbon bond distance of 1.192(24) Å. Costain uncertainties are given in parentheses for each bond distance. These large uncertainties in the bond distance are propagated from the large Costain error obtained from the small carbonyl carbon *b* coordinate (*14*). The substitution carbon–carbon bond distance in ketene also has a large uncertainty due to a similar small coordinate problem (*15*).

The structure with a tilt of the argon atom toward the carbonyl carbon of ketene suggests an assignment of the observed spectrum of HDCCO–Ar to the structural isotopomer that places the deuterium adjacent to the argon atom (designated IIa in Fig. 2 for a planar form). The experimental rotational constants of HDCCO–Ar are in better agreement with those calculated for IIa than with those for IIb using the structure described above, where it is found that $R_{cm} = 3.5868(3)$ Å and $\theta_{cm} = 96.4^\circ(2)$. With this structural assignment of HDCCO–Ar, it is interesting to see how the inclusion of the moments of inertia of HDCCO–Ar and D_2CCO–Ar affect the least squares fit described above which includes only the normal and carbon-13 moment of inertia data. Since the inertial defects of HDCCO–Ar and D_2CCO–Ar decrease by 0.10605 and 0.50725 uÅ^2, respectively, from that of H_2CCO–Ar, the zero point vibrational effects due to deuterium substitution are expected to be large. These effects should increase the overall standard deviations of the least squares fits and this is found to be the case. A least squares fit using I_{aa} and I_{cc} of H_2CCO–Ar, $H_2C^{13}CO$–Ar, $H_2{}^{13}CCO$–Ar and HDCCO–Ar beginning at $\theta_{cm} \geq 90^\circ$ converges to $R_{cm} = 3.590(3)$ Å and $\theta_{cm} = 97.3^\circ(1.6)$ with an overall standard deviation of $\sigma = 0.83$ uÅ^2. Although the standard deviation of this fit is quite large, the values of R_{cm} and θ_{cm} are in agreement with the best fit (where $R_{cm} = 3.5868$ Å and $\theta_{cm} = 96.4^\circ$). When I_{aa} and I_{cc} of D_2COO–Ar are also included in the least squares fit, the standard deviation increases to $\sigma = 1.24$ uÅ^2. However, it is found $R_{cm} = 3.587(4)$ Å and $\theta_{cm} = 95^\circ(3)$ which is still in good agreement with the best fit.

Further evidence for the large zero point vibrational effects upon substitution of deuterium for hydrogen in the complex come from a calculation of the substitution C–H bond distance. A value of 0.552 Å (*11*) is determined for this distance from the moments of inertia of H_2CCO–Ar and HDCCO–Ar using Rudolph's equations (*14*). This unrealistic value may be compared to the normal C–H bond distance of 1.0905 Å found for ketene (*15*). There are no small coordinates or ambiguities associated with the signs of the atomic coordinates to complicate the calculation and the discrepancy is due to the large zero point effects noted above for deuterium.

Since the rotational constants of the A_2 state are well-determined from the spectroscopic analysis, analogous least squares fits of the moments of inertia of the H_2CCO–Ar, $H_2C^{13}CO$–Ar, and $H_2{}^{13}CCO$–Ar isotopomers to R_{cm} and θ_{cm} were done to determine whether the effective structure differs in the two tunneling states. From the fit of I_{aa} and I_{cc}, it was found that $R_{cm} = 3.5784(3)$ Å and $\theta_{cm} = 95.8^\circ(2)$ with an overall standard deviation of $\sigma = 0.079$ uÅ^2. Thus, structures derived from the effective moments of inertia of the A_1 and A_2 states are not significantly different.

VI. VAN DER WAALS STRETCHING FORCE CONSTANT

An estimate of the van der Waals stretching force constant was obtained from the quartic centrifugal distortion constant, Δ_J, of the A_1 state of H_2CCO–Ar using

$$k_s = 64\pi^4 m_r^2 R_{cm}^2 (B^4 + C^4)/h\Delta_J. \qquad [4]$$

Millen gives this equation for a planar asymmetric top complex (*20*). The rotational constants, *B* and *C*, were taken from Table 4, $R_{cm} = 3.587$ Å, and m_r is the pseudodiatomic reduced mass defined in Eq. [2]. Using these values in Eq. [4] gives $k_s = 1.699$ N/m (0.01699 mdyne/Å).

VII. INTERNAL MOTION

There is considerable spectral evidence that the A_1 and A_2 states of H_2CCO–Ar arise from tunneling of the protons between two equivalent frameworks. Pure *a*- and *b*-type rotational transitions are observed for the two states as expected for proton exchange through rotation about the C=C=O axis of ketene. Nuclear spin statistical weights observed for H_2CCO–Ar, $H_2C^{13}CO$–Ar, $H_2{}^{13}CCO$–Ar, and D_2CCO–Ar, in addition to the resolution of the $I = 0$, 2 and $I = 1$ nuclear deuterium spin states in D_2CCO–Ar, provide definitive evidence that the states arise from tunneling motion of the protons and deuterons. The electric dipole moments of the two states are almost the same as expected for an interconversion path about the two-fold axis of ketene. Also, the tunneling splittings are reduced by a factor of approximately 5 to 10 upon deuteration (see Tables 1 and 2 for the splittings of the H_2CCO–Ar and D_2CCO–Ar transitions). Although the rotational constants differ between the two states,

the effective structures are virtually the same as determined from least squares fits of the moment of inertia. Since only one set of rotational transitions is observed for HDCCO–Ar, the motion is quenched for a planar complex. This evidence is consistent with the structural results derived from fits of the effective moments of inertia and it supports arguments for a planar structure. Finally, several observations indicate the barrier to internal rotation is not low. The two tunneling state transition frequencies for each isotopomer fit within experimental error to a semirigid Hamiltonian, and the tunneling splittings for the transitions are relatively small.

VIII. DISCUSSION

Ar–ketene and Ar–formaldehyde both have T-shaped, planar structures and exhibit two internal rotor states due to tunneling of the two hydrogen atoms (*3*). It is likely that the barrier to internal rotation is not low for the two complexes since the Ar–formaldehyde transitions of both states, like Ar–ketene, fit to a semirigid rotor Hamiltonian and the tunneling splitting varies from several MHz to over 100 MHz (*3*). Using Eq. [4] with the reported spectral constants of the ground state of H_2CO–Ar (*3*), the van der Waals stretching force constant, k_s, is found to be 1.307 N/m · H_2CCO–Ar has a k_s value of 1.699 N/m and this suggests that the binding is stronger in the ketene complex.

The effective geometries of the two internal rotor states of Ar–ketene do not differ significantly. The preferred values of the structural parameters are $R_{cm} = 3.587$ Å and $\theta_{cm} = 96.4^\circ$ for the A_1 state and $R_{cm} = 3.578$ Å and $\theta_{cm} = 95.8^\circ$ for the A_2 state. Consequently, both states have argon tilted by approximately 6° toward the carbonyl carbon of ketene. The variation in the structure which was determined by the least squares fits of various combinations of the moments of inertia of the isotopomers of Ar– ketene indicates that the effective R_{cm} distance and θ_{cm} angle have uncertainties of 0.01 Å and 1°. However, the tilt is small and it is difficult to extrapolate to an equilibrium geometry given the large amplitude in-plane bending likely to be present in the complex.

The effective tilt of formaldehyde with respect to argon is not unambiguously determined from the published moment of inertia data. Least squares fits of the moments of inertia I_a, I_b, and I_c of H_2CO–Ar and D_2CO–Ar give $R_{cm} = 3.650(5)$ Å and $\theta_{cm} = 93.0^\circ(47)$ for the A_1 state (designated S in Ref. *3*) and $R_{cm} = 3.658(4)$ Å and $\theta_{cm} = 79.7^\circ(44)$ for the A_2 state (designated T in Ref. *3*). When different combinations of two moments of inertia for each isotopomer are fit to R_{cm} and θ_{cm}, it is found that θ_{cm} varies between 81° and 101° for the A_1 state and R_{cm} varies form 3.640 Å to 3.659 Å. Similar results are obtained for the A_2 state of Ar–formaldehyde. The *A* rotational constant is not well determined for D_2CO–Ar due to the lack of assigned *b*-type transitions. However, changing *A* by one standard deviation has little effect upon the least squares fits described above. Rotational spectra of carbon-13 and oxygen-18 isotopomers are needed to determine the effective tilt of formaldehyde with respect to argon.

TABLE 10
Comparison of van der Waals Parameters of Argon Complexes

Complex	k_s (mdynes/Å)[a]	R_{cm} (Å)[b]	θ_{cm} (°)[b]	Δ (amuÅ^2)[c]	Reference
OCS-Ar	0.0222	3.699	108.1	2.83	21, 23
NNO-Ar	0.0194	3.470	97.4	2.28	22
H_2CCO-Ar	0.0170	3.587	96.4	2.67	this work
H_2CO-Ar	0.0131	3.659		2.27	4
CO-Ar		3.811	109.8	8.45	23

[a] The van der Waals stretching force constant; see references and text for method of calculation.

[b] The structural parameters are defined in Fig. 1; for each complex, θ_{cm} is defined as the angle between the line connecting argon with the center of mass of the molecule and the a' axis of the molecule in the direction toward the heavy atom at the end opposite to the oxygen.

[c] $\Delta = I_c - I_b - I_a$ is the inertia defect of the ground state of the normal isotopomer.

Table 10 compares van der Waals parameters of several T-shaped argon complexes with Ar–ketene and Ar–formaldehyde. The structure listed for Ar–formaldehyde was determined from a least squares fit of I_{aa} and I_{cc} for the H_2CO–Ar and D_2CO–Ar isotopomers in order to be consistent with the method used to obtain the Ar–ketene structure. Smaller R_{cm} for OCS–Ar (*21*), NNO–Ar (*22*), H_2CO–Ar (*3*), and H_2CCO–Ar suggest that these complexes are more tightly bound than CO–Ar (*23*). The unusually large positive inertial defect also indicates very large amplitude bending motion in CO–Ar compared to the other complexes (*23*). In Table 10 the increase in the van der Waals stretching force constant, k_s, from H_2CO–Ar to OCS–Ar can be qualitatively rationalized by the expected increase in the molecular electric polarizability as the number of electrons increases in the molecule. This should lead to an increase in the van der Waals interaction between the argon atom and the molecule and hence an increase in the van der Waals stretching force constant. T-shaped structures in which the argon atom is tilted toward the oxygen end of the molecule are found for OCS–Ar, NNO–Ar, H_2CCO–Ar, and CO–Ar.

REFERENCES

1. C. W. Gillies, J. Z. Gillies, F. J. Lovas, and R. D. Suenram, *J. Am. Chem. Soc.* **115,** 9253–9262 (1993).
2. F. J. Lovas, R. D. Suenram, C. W. Gillies, J. Z. Gillies, P. W. Fowler, and Z. Kisiel, *J. Am. Chem. Soc.* **116,** 5285–5294 (1994).
3. S. E. Novick, *J. Chem. Phys.* **99,** 7506–7509 (1993).
4. J. Sadlej, M. M. Szczesniak, and G. Chalasinski, *J. Chem. Phys.* **99,** 5211–5218 (1993).
5. J. Z. Gillies, C. W. Gillies, J.-U. Grabow, H. Hartwig, and E. Block, *J. Phys. Chem.* **100,** 18 708–18 717 (1996).
6. J.-U. Grabow, W. Stahl, *Z. Naturforsch. A* **45,** 1043–1046 (1990).

7. C. W. Boyce, C. W. Gillies, H. Warner, J. Z. Gillies, F. J. Lovas, and R. D. Suenram, *J. Mol. Spectrosc.* **171,** 533–545 (1995).
8. J. M. L. J. Reinhartz and A. Dymanus, *Chem. Phys. Lett.* **24,** 346–347 (1974).
9. A. D. Jenkins, *J. Chem. Soc.*, 2563–2568 (1952).
10. A. P. Cox and A. S. Esbitt, *J. Chem. Phys.* **38,** 1636–16 (1963).
11. J. K. G. Watson, *in* "Vibrational Spectra and Structure" (J. R. Durig, Ed.), Vol. 6, p. 1. Elsevier, Amsterdam, 1977.
12. L. H. Coudert, d2 least squares fit program.
13. K. Matsumura, F. J. Lovas, and R. D. Suenram, *J. Chem. Phys.* **91,** 5887–5894 (1989).
14. W. Gordy and R. L. Cook, "Microwave Molecular Spectra." Wiley, New York, 1984.
15. R. D. Brown, P. D. Godfrey, D. McNaughton, A. P. Pierlot, and W. H. Taylor, *J. Mol. Spectrosc.* **140,** 340–352 (1990).
16. B. Fabricante, D. Krieger, and J. S. Muenter, *J. Chem. Phys.* **67,** 1576–1586 (1977).
17. M. R. Keenan, D. B. Wozniak, and W. Flygare, *J. Chem. Phys.* **75,** 631–640 (1981).
18. S. J. Harris, K. C. Janda, S. E. Novick, and W. Klemperer, *J. Chem. Phys.* **63,** 881–884 (1975).
19. J. M. Steed, T. A. Dixon, and W. Klemperer, *J. Chem. Phys.* **70,** 4095–4100 (1979).
20. D. J. Millen, *Can. J. Chem.* **63,** 1477–1479 (1985).
21. Y. Xu, W. Jaeger, and M. C. L. Gerry, *J. Mol. Spectrosc.* **151,** 206–216 (1992).
22. C. H. Joyner, T. A. Dixon, F. A. Baiocchi, and W. Klemperer, *J. Chem. Phys.* **75,** 5285–5290 (1981).
23. T. Ogata, W. Jager, I. Ozier, and M. C. L. Gerry, *J. Chem. Phys.* **98,** 9399–9409 (1993).